also shows that $\eta$ is of the order of $10^{-5}$ with $\epsilon=0.1$. Since $P_T^B$ is proportional to $(A_f/\lambda_l^2)^2$, either increasing $\epsilon$ or changing the surface contour $f(x)$, according to (30), $A_f$ may be increased giving a larger $\eta$.

It is clear from the example that we may achieve the control of the surface-to-bulk wave conversion process by carefully designing the region of discontinuity. The application of this analysis to the tapping of surface wave in isotropic media remains to be checked by experiments.

## References


[1] R. C. McMaster, Ed., *Nondestructive Testing Handbook*. New York: Ronald, 1963.
[2] E. G. Cook and H. E. Van Valkenburg, "Surface waves at ultrasonic frequencies," *Amer. Soc. Test. Mater. Bull.*, TP127, pp. 81–84, May 1954.
[3] E. A. Ash, R. M. De La Rue, and R. F. Humphryes, "Microsound surface waveguides," *IEEE Trans. Microwave Theory Tech. (Special Issue on Microwave Acoustics)*, vol. MTT-17, pp. 882–892, Nov. 1969.
[4] H. L. Bertoni, "Piezoelectric Rayleigh wave excitation by bulk wave scattering," *IEEE Trans. Microwave Theory Tech. (Special Issue on Microwave Acoustics)*, vol. MTT-17, pp. 873–882, Nov. 1969.
[5] R. F. Humphryes and E. A. Ash, "Acoustic bulk surface wave transducers," *Electron. Lett.*, vol. 5, pp. 175–176, May 1969.
[6] P. M. Morse and H. Feshback, *Methods of Theoretical Physics*, vol. 2. New York: McGraw-Hill, 1953, ch. 9.
[7] Y. M. Chen and S. J. Kim, "Scattering of acoustic waves by a penetrable sphere with statistically corrugated surface," *J. Acoust. Soc. Amer.*, vol. 42, pp. 1–5, July 1967.
[8] R. E. Collin, *Field Theory of Guided Waves*. New York: McGraw-Hill, 1960, ch. 11.
[9] B. A. Auld, "Application of microwave concepts to the theory of acoustic fields and waves in solids," *IEEE Trans. Microwave Theory Tech. (Special Issue on Microwave Acoustics)*, vol. MTT-17, pp. 800–811, Nov. 1969.


# Elastic Waves Guided by a Solid Layer Between Adjacent Substrates

ROBERT C. M. LI, MEMBER, IEEE, AND KUO-HSIUNG YEN

***Abstract*—The present investigation is motivated by the problem of coupling Rayleigh waves between adjacent substrates when either substrate is nonpiezoelectric, in which case it becomes necessary to resort to some mechanical means to achieve this coupling. The use of a fluid coupling layer has been investigated and experimentally demonstrated elsewhere, while the use of a solid layer, with its inherently greater mechanical stability, has also been proposed. In this work, the operating characteristics of a specific solid-layer structure are predicted on the basis of a theoretical analysis, which furnishes the propagation characteristics and field structure of the waves which may be guided by a solid layer between two identical solids.**

## I. Introduction

THE present investigation is motivated by the problem of transferring the energy in an acoustic Rayleigh wave propagating on the surface of a given substrate to the Rayleigh wave on an adjacent substrate. In the absence of any guiding mechanism, the total time delay available on an acoustic-surface-wave delay line is limited by the length of the crystal substrate, but such a limitation may be overcome by coupling the Rayleigh wave from the surface of one substrate to that of an adjacent substrate, thus lengthening the total delay path.

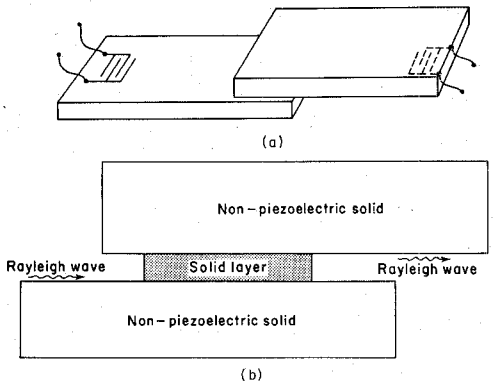


Fig. 1. Coupling of Rayleigh waves between (a) piezoelectric substrates by means of an air gap and (b) nonpiezoelectric substrates by means of a solid layer.

When a Rayleigh wave is generated on a piezoelectric substrate, coupling to the Rayleigh wave on an adjacent piezoelectric substrate can be effected via the evanescent electric field in the air gap when the two substrates are brought close together [1], as shown in Fig. 1(a). If the adjacent substrate is not piezoelectric, however, this method is no longer feasible and an alternative scheme must be employed. Such a scheme has recently been proposed and experimentally demonstrated [2], [3],

Manuscript received September 2, 1971; revised October 26, 1971. This work was supported by the U. S. Army Electronics Command, Fort Monmouth, N. J., under Contract DAAB07-69-C-0418. It is based on part of a dissertation to be submitted by K. H. Yen to the Department of Electrical Engineering and Electrophysics, Polytechnic Institute of Brooklyn, Farmingdale, N. Y., in partial fulfillment of the requirements for the Ph.D. degree.

The authors are with the Department of Electrical Engineering and Electrophysics, Polytechnic Institute of Brooklyn, Farmingdale, N. Y. 11735.

the coupling under these conditions being achieved by inserting a layer of fluid or solid between the two substrates, and the energy transferred via the mechanical rather than electric field.

A schematic diagram of the physical arrangement employing a solid layer is shown in Fig. 1(b). Broadly speaking, the principle of operation of this device is the same for both fluid and solid coupling layers. Referring to Fig. 1(b), the configuration may be divided into three distinct regions, each capable of supporting its own spectrum of modes or guided waves. The first of these regions is the original substrate supporting the generated Rayleigh wave, which of course is the mode of that free surface. The second region consists of a layered configuration which is capable of supporting an infinite number of modes guided along the direction of the interface. And finally, there is the free surface of the second substrate, onto which elastic energy is to be coupled, again in the form of its Rayleigh wave mode. The operation of the device can therefore be understood in terms of the initial Rayleigh wave being incident on the layered system and exciting all of the characteristic modes thereof. Those which are above cutoff are then guided to the other end of the layered region, and similarly reconverted into a Rayleigh wave, both on the original substrate and also on the adjacent substrate.

For a detailed understanding of the coupling behavior, as well as for design purposes, a knowledge of the dispersion characteristics of the layered configuration is essential. For the case of a fluid layer, results have already been obtained and are presented in [3]. The objective of this investigation is the analysis of the dispersion characteristics and the modal fields of the solid-layer configuration.

## II. Modes of a Solid Layer Between Two Solids

Two kinds of modes can exist in the solid-layer region of Fig. 1(b), one of the Rayleigh type with particle velocity in the sagittal plane, and the other of the Love or SH type with particle velocity perpendicular to the sagittal plane. Of these two, only the Rayleigh type is relevant to the coupling of Rayleigh waves between adjacent substrates since the Love type of mode is orthogonal in polarization to the Rayleigh wave. For the sake of completeness, however, the properties of both mode types will be investigated.

For the purposes of analysis, the layered region in the structure of Fig. 1(b) is idealized as a solid elastic layer between two identical half-spaces, as shown in Fig. 2. For the sake of simplicity and with no loss in generality, it is assumed that the fields do not vary in $y$, so that $k_y=0$ and $k_t=\sqrt{k_x^2+k_y^2}=k_x$.

In solving for the modes of this layered configuration, it is convenient to employ a microwave network approach first described in [4], and subsequently elaborated on in more detail in [5]–[7]. In the context of the present problem, this involves the representation of the bulk wave constituents which comprise the modal fields

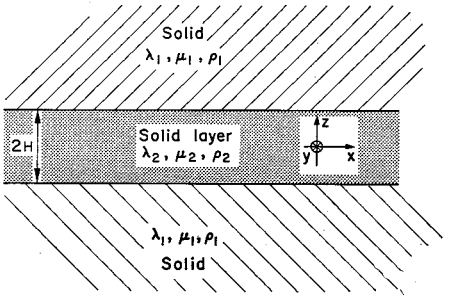


Fig. 2. Model for analysis of modes guided by a solid layer between two substrates.

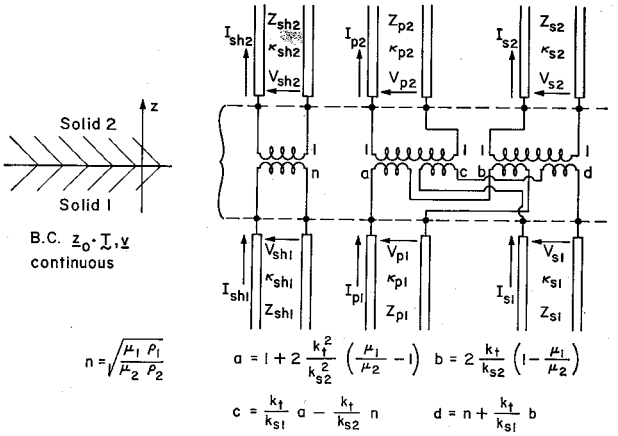


Fig. 3. Equivalent network for solid–solid interface.

in the substrate and layer regions in terms of transmission lines, and the representation of the solid–solid interfaces in terms of equivalent networks which couple the aforementioned transmission lines. In addition, it is convenient to choose the direction of the transmission lines to coincide with the transverse $z$ direction (perpendicular to the interfaces), in order to obtain a *transverse* equivalent network, to which one may then apply the transverse resonance condition and so obtain the dispersion relation for the modes of the configuration. The virtue of this approach lies in the fact that all of the elements required, namely, the transmission line representations for the bulk wave constituents and the equivalent network for the solid–solid interface, have been previously derived [6], [7], and it is a trivial matter to combine these various building-blocks in the appropriate manner to obtain the transverse equivalent network for the structure at hand. For convenience, the parameters of the respective transmission line representations and their associated mode functions are shown in Table I, and the equivalent network for a solid–solid interface is shown in Fig. 3. The parameters which describe the properties of an isotropic elastic medium are the density $\rho$, the rigidity $\mu$, and the compressibility $\lambda$. In terms of these parameters, the wavenumbers of plane bulk waves are given by

$$k_p=\omega\sqrt{\frac{\rho}{\lambda+2\mu}} \qquad k_s=\omega\sqrt{\frac{\rho}{\mu}} \tag{1}$$

where the subscripts $p$ and $s$ denote compressional ($P$)

TABLE I

CHARACTERISTIC IMPEDANCES AND MODE FUNCTIONS FOR PLANE BULK WAVES

a) *P* Wave in a Fluid

$$Z_f = \frac{\omega\rho_f}{\kappa_f} \qquad \kappa_f = \sqrt{k_f^2 - k_t^2}$$

$$\boldsymbol{g} = \begin{bmatrix} k_x/\omega\rho_f \\ k_y/\omega\rho_f \\ -1 \end{bmatrix} \qquad \boldsymbol{q} = \begin{bmatrix} 0 \\ 0 \\ 1 \end{bmatrix}$$

$$t_{xx} = -1$$
$$t_{xy} = 0$$
$$t_{yy} = -1$$

b) *P* Wave in a Solid

$$Z_p = \frac{\omega\rho}{\kappa_p} \qquad \kappa_p = \sqrt{k_p^2 - k_t^2}$$

$$\boldsymbol{g} = \begin{bmatrix} k_x/\omega\rho \\ k_y/\omega\rho \\ -\left(1 - 2\frac{k_t^2}{k_s^2}\right) \end{bmatrix} \qquad \boldsymbol{q} = \begin{bmatrix} -2\omega\rho k_x/k_s^2 \\ -2\omega\rho k_y/k_s^2 \\ 1 \end{bmatrix}$$

$$t_{xx} = -\left(\frac{\lambda}{\lambda + 2\mu} + \frac{2k_x^2}{k_s^2}\right)$$
$$t_{xy} = -2\frac{k_x k_y}{k_s^2}$$
$$t_{yy} = -\left(\frac{\lambda}{\lambda + 2\mu} + \frac{2k_y^2}{k_s^2}\right)$$

c) *SV* Wave in a Solid

$$Z_s = \frac{\mu\kappa_s}{\omega} \qquad \kappa_s = \sqrt{k_s^2 - k_t^2}$$

$$\boldsymbol{g} = \begin{bmatrix} -\frac{k_s k_x}{\omega\rho k_t} \\ -\frac{k_s k_y}{\omega\rho k_t} \\ -\frac{2k_t}{k_s} \end{bmatrix} \qquad \boldsymbol{q} = \begin{bmatrix} \omega\rho\frac{k_x}{k_s k_t}\left(1 - 2\frac{k_t^2}{k_s^2}\right) \\ \omega\rho\frac{k_y}{k_s k_t}\left(1 - 2\frac{k_t^2}{k_s^2}\right) \\ \frac{k_t}{k_s} \end{bmatrix}$$

$$t_{xx} = 2\frac{k_x^2}{k_s k_t}$$
$$t_{xy} = 2\frac{k_x k_y}{k_s k_t}$$
$$t_{yy} = 2\frac{k_y^2}{k_s k_t}$$

d) *SH* Wave in a Solid

$$Z_{sh} = \frac{\omega\rho}{\kappa_s} \qquad \kappa_s = \sqrt{k_s^2 - k_t^2}$$

$$\boldsymbol{g} = \begin{bmatrix} -\frac{k_s k_y}{\omega\rho k_t} \\ \frac{k_s k_x}{\omega\rho k_t} \\ 0 \end{bmatrix} \qquad \boldsymbol{q} = \begin{bmatrix} \omega\rho\frac{k_y}{k_s k_t} \\ -\omega\rho\frac{k_x}{k_s k_t} \\ 0 \end{bmatrix}$$

$$t_{xx} = 2\frac{k_x k_y}{k_s k_t}$$
$$t_{xy} = \frac{k_y^2 - k_x^2}{k_s k_t}$$
$$t_{yy} = -2\frac{k_x k_y}{k_s k_t}$$

and shear ($S$) waves, respectively. The total transverse (to $z$) wavenumber is denoted by

$$k_t = \sqrt{k_x^2 + k_y^2}. \tag{2}$$

In Table I, the modal quantities are listed for the pressure ($P$) waves of a fluid and the $P$, $SV$, and $SH$ waves in an isotropic solid. The subscripts $f$, $p$, $s$, and $sh$ refer, respectively, to fluid, $P$ waves, $SV$ waves, and $SH$ waves.

For each mode, the table includes the characteristic impedance $Z$ and the wavenumber $\kappa$ of its transmission line representation, as well as the mode functions ($1\times3$ matrices) $\boldsymbol{g}$ and $\boldsymbol{q}$, from which the components of the particle velocity $\boldsymbol{v}$ and the stress vector $\boldsymbol{z}_0\cdot\mathfrak{I}$ can be found from the relations

$$\boldsymbol{G}(x, y, z) = \begin{bmatrix} v_x(\boldsymbol{r}) \\ v_y(\boldsymbol{r}) \\ T_{zz}(\boldsymbol{r}) \end{bmatrix} = V(z)\boldsymbol{g}e^{-j(k_x x + k_y y)} \tag{3}$$

and

$$\boldsymbol{Q}(x, y, z) = \begin{bmatrix} T_{xz}(\boldsymbol{r}) \\ T_{yz}(\boldsymbol{r}) \\ v_z(\boldsymbol{r}) \end{bmatrix} = I(z)\boldsymbol{q}e^{-j(k_x x + k_y y)} \tag{4}$$

where $V(z)$ and $I(z)$ are the modal voltage and current of the transmission line representation. The three additional components of stress $T_{xx}$, $T_{xy}$, and $T_{yy}$ can be found from

$$\begin{bmatrix} T_{xx}(\boldsymbol{r}) \\ T_{xy}(\boldsymbol{r}) \\ T_{yy}(\boldsymbol{r}) \end{bmatrix} = V(z)\begin{bmatrix} t_{xx} \\ t_{xy} \\ t_{yy} \end{bmatrix} e^{-j(k_x x + k_y y)} \tag{5}$$

where $t_{xx}$, $t_{xy}$, and $t_{yy}$ are also given in the table.

With the information contained in Table I and Fig. 3, it is possible to derive the propagation characteristics and the field structure of modes which can be guided by the solid-layer structure of Fig. 2.

### *A. Rayleigh-Type Modes*

In order to efficiently couple from a Rayleigh wave to waves of the layered region and vice versa, the properties of the solids in Fig. 2 are chosen so that the shear wave velocity in the layer is less than that in the half spaces, in which case the modes are bound to and guided along the layer, but decaying into the half spaces over most of the frequency range. Although there has been some earlier work on this configuration [8], it does not seem to be readily accessible. A more recent work [9] formulates the more general problem where the adjacent half-spaces are not identical, but does not furnish any numerical results.

*1) Dispersion Relations:* The method of analysis employed here consists of formulating a transverse equivalent network for the structure of Fig. 2, and then applying the familiar transverse resonance technique. For the Rayleigh type of modes considered in this section, the modal fields are made up of bulk $P$ and $SV$ waves which combine together to satisfy the

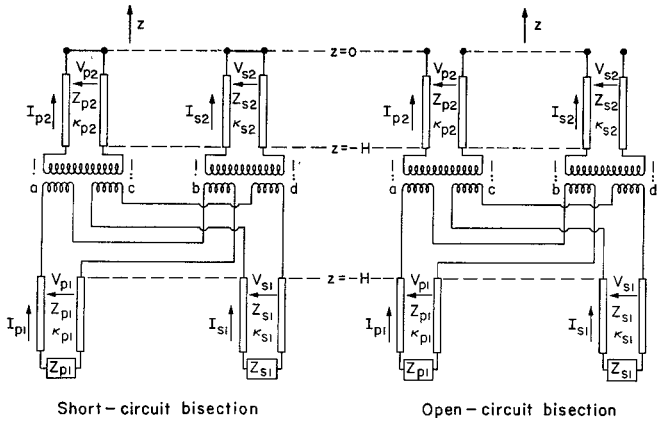


Fig. 4. Open-circuit and short-circuit bisections of transverse equivalent network for Rayleigh-type modes of a solid layer between identical half-spaces. The former corresponds to even modes and the latter to odd modes.

boundary conditions at the solid–solid interfaces. Hence, the transverse equivalent network will consist of two transmission lines, one representing a $P$ wave and the other a $SV$ wave, in each of the two substrate regions as well as in the layer region, and the lines of the layer region are then coupled to those of the substrate regions by a coupling network representing a solid–solid interface at each interface plane. In view of the reflection symmetry of the structure about the midplane $z=0$, however, the characteristic modes are either even or odd about the midplane and these then correspond, respectively, to the free resonances of the open-circuit and short-circuit bisections of the symmetric transverse equivalent network, which bisections are shown in Fig. 4.

In the above equivalent networks, the condition for the existence of free resonances corresponds to the condition for the existence of guided waves on the physical structure, and this condition is the transverse resonance condition [10]:

$$\det (\overleftarrow{\mathbf{Z}} + \overrightarrow{\mathbf{Z}}) = 0 \tag{6}$$

where $\overleftarrow{\mathbf{Z}}$ and $\overrightarrow{\mathbf{Z}}$ are the impedance matrices seen looking in opposite directions at any reference plane $T$ in the network. The application of (6) to the two bisected networks of Fig. 4 then yields the dispersion relations for the even and odd modes. As shown in the following derivation, the resonance condition for both bisections or, equivalently, the dispersion relation for modes of both symmetries, can be obtained from a single unified derivation. To this end, choose the reference plane $T$ to coincide with the plane $z=-H$ in the substrate region. Let $\mathbf{Z}(-H)$ be the impedance matrix looking into the semi-infinite substrate region. Then

$$\overleftarrow{\mathbf{Z}}(-H) = \begin{bmatrix} Z_{p1} & 0 \\ 0 & Z_{s1} \end{bmatrix}. \tag{7}$$

In order to derive $\overrightarrow{\mathbf{Z}}(-H)$, the impedance matrix seen looking in the other direction at this reference plane, we note from the transformer coupling network that the terminal voltages are related by

$$\begin{bmatrix} V_{p1} \\ V_{s1} \end{bmatrix} = \begin{bmatrix} a & b \\ c & d \end{bmatrix} \begin{bmatrix} V_{p2} \\ V_{s2} \end{bmatrix} = \begin{bmatrix} a & b \\ c & d \end{bmatrix} \begin{bmatrix} \hat{Z}_{p2} I_{p2} \\ \hat{Z}_{s2} I_{s2} \end{bmatrix} \tag{8}$$

where

$$\hat{Z}_{p2} = jZ_{p2} \tan \kappa_{p2} H \tag{9a}$$

$$\hat{Z}_{s2} = jZ_{s2} \tan \kappa_{s2} H \tag{9b}$$

for the short-circuit bisection and

$$\hat{Z}_{p2} = -jZ_{p2} \cot \kappa_{p2} H \tag{10a}$$

$$\hat{Z}_{s2} = -jZ_{s2} \cot \kappa_{s2} H \tag{10b}$$

for the open-circuit bisection. Similarly, the terminal currents are related by

$$\begin{bmatrix} I_{p2} \\ I_{s2} \end{bmatrix} = \begin{bmatrix} a & c \\ b & d \end{bmatrix} \begin{bmatrix} I_{p1} \\ I_{s1} \end{bmatrix}. \tag{11}$$

Combining (11) and (8), one has

$$\begin{bmatrix} V_{p1} \\ V_{s1} \end{bmatrix} = \begin{bmatrix} a & b \\ c & d \end{bmatrix} \begin{bmatrix} \hat{Z}_{p2} & 0 \\ 0 & \hat{Z}_{s2} \end{bmatrix} \begin{bmatrix} a & c \\ b & d \end{bmatrix} \begin{bmatrix} I_{p1} \\ I_{s1} \end{bmatrix} \tag{12}$$

from which it follows that

$$\begin{aligned} \overrightarrow{\mathbf{Z}}(-H) &= \begin{bmatrix} a & b \\ c & d \end{bmatrix} \begin{bmatrix} \hat{Z}_{p2} & 0 \\ 0 & \hat{Z}_{s2} \end{bmatrix} \begin{bmatrix} a & c \\ b & d \end{bmatrix} \\ &= \begin{bmatrix} a^2\hat{Z}_{p2} + b^2\hat{Z}_{s2} & ac\hat{Z}_{p2} + bd\hat{Z}_{s2} \\ ac\hat{Z}_{p2} + bd\hat{Z}_{s2} & c^2\hat{Z}_{p2} + d^2\hat{Z}_{s2} \end{bmatrix}. \end{aligned} \tag{13}$$

Substituting (7) and (13) into (6), one obtains the desired dispersion relation

$$\begin{aligned} &(a^2\hat{Z}_{p2} + b^2\hat{Z}_{s2} + Z_{p1})(c^2\hat{Z}_{p2} + d^2\hat{Z}_{s2} + Z_{s1}) \\ &\qquad - (ac\hat{Z}_{p2} + bd\hat{Z}_{s2})^2 = 0 \end{aligned} \tag{14}$$

where $\hat{Z}_{p2}$ and $\hat{Z}_{s2}$ are defined for odd and even modes in (9) and (10), respectively, the various characteristic impedances $Z_{si}$ and $Z_{pi}$ for the two regions $i=1, 2$ are defined in Table I, and the coupling network parameters $a$, $b$, $c$, and $d$ are defined in Fig. 3. Equation (14) is an implicit equation for the modal wavenumber $k_x$ as a function of the angular frequency $\omega$; it applies to odd modes upon use of (9) and to even modes upon use of (10).

The type of solutions sought corresponds to fields which are transversely decaying into the substrates and hence characterized by imaginary wavenumbers $\kappa_{p1}$ and $\kappa_{s1}$ for the respective $P$ and $SV$ wave constituents in the substrates. In the layer, on the other hand, the fields are generally transversely propagating, but it is possible for the $P$ wave to become cutoff transversely (with hyperbolic rather than trigonometric variation in $z$) without altering the basic nature of the wave as long as the $SV$ wave is still transversely propagating, in the sense that most of the energy is still confined to the layer region and attenuates into the substrates.

*2) Numerical Solution of Dispersion Relations:* The numerical solution of the dispersion relation (14) is

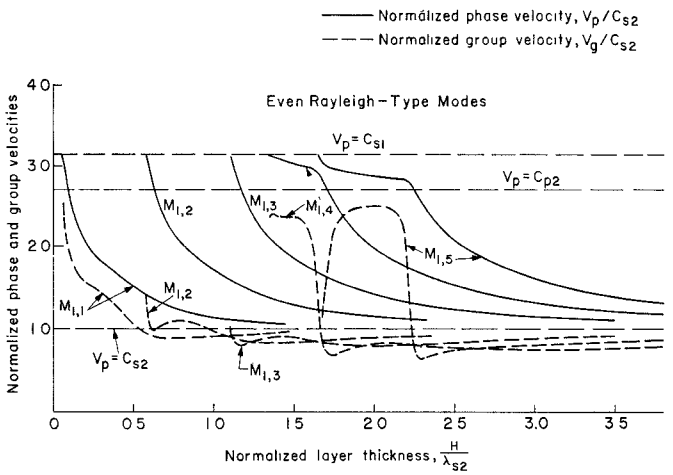


Fig. 5. Dispersion characteristics of even Rayleigh-type modes in gold layer between fused quartz substrates.

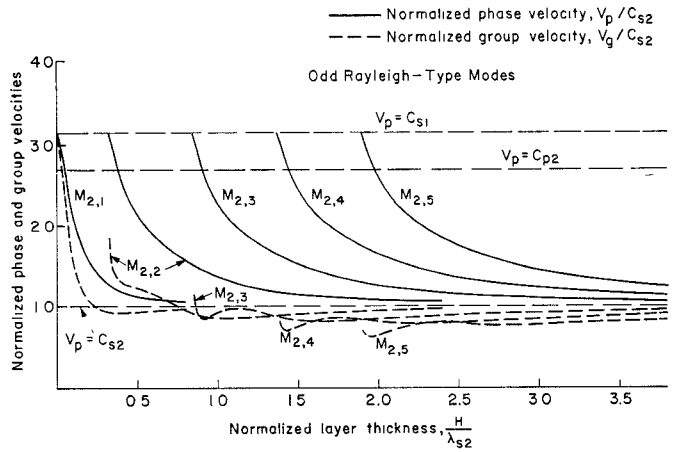


Fig. 6. Dispersion characteristics of odd Rayleigh-type modes in gold layer between fused quartz substrates.

shown in Figs. 5 and 6 for several of the lower modes of each symmetry, for the case of a gold layer between two fused quartz substrates. The phase velocity $v_p$ and group velocity $v_g$ are normalized to $C_{s2}$, the shear-wave velocity in the layer, and these velocities are plotted as a function of $H/\lambda_{s2}$, where $H$ is half the layer thickness and $\lambda_{s2}$ is the wavelength of shear waves in the layer. The phase and group velocities are related to the guided-wave wavenumber $k_x$ in the standard fashion

$$v_p = \frac{\omega}{k_x} \qquad v_g = \frac{d\omega}{dk_x}. \tag{15}$$

The region of real solutions is bounded by $C_{s2}$ and $C_{s1}$, the shear-wave velocities in the layer and substrate, respectively. This region may be subdivided into two portions separated by $C_{p2}$, the longitudinal-wave velocity in the layer. For $C_{p2} < v_p < C_{s1}$, all of the modes are such that the $P$ and $SV$ wave constituents are transversely propagating in the layer. For $C_{s2} < v_p < C_{p2}$, however, the $P$ wave constituent in the layer is transversely below cutoff, so that the transverse dependence of the fields is a combination of a trigonometric variation for the $SV$ wave constituent and a hyperbolic

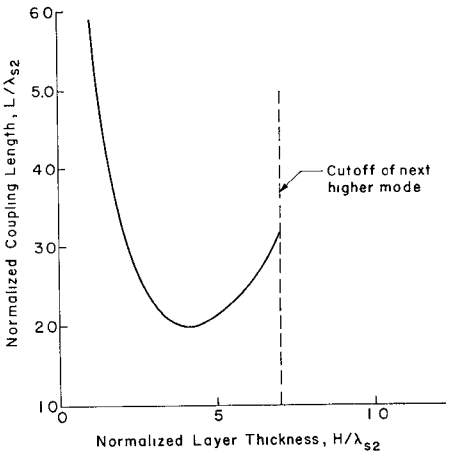


Fig. 7. Nominal coupling length of solid layer required for total transfer of Rayleigh wave between substrates.

variation for the $P$ wave constituent. Throughout the entire region of real solutions, however, the bulk wave constituents in the substrate regions are purely evanescent, in the transverse $z$ direction.

In the limit of a vanishingly thin layer ($H/\lambda_{s2} \to 0$), the phase velocity reduces to that of a shear wave in the substrate, as expected. Similarly, in the limit of an infinitely thick layer, the phase velocity approaches that of a shear wave in the layer.

*3) Design of Coupling Layer:* From the dispersion curves $M_{1,1}$ and $M_{2,1}$ for the lowest even and odd modes, respectively, one may calculate a coupling length $L$ required for the optimum transfer of the Rayleigh wave from one substrate to a second identical substrate by means of the well-known directional-coupler formula:

$$(k_{xo} - k_{xe})L = \pi \tag{16}$$

where $k_{xe}$ and $k_{xo}$ are the wavenumbers of the lowest even and odd modes, respectively. The validity of (16) is discussed in the Appendix.

Equation (16) may be written in normalized form as follows:

$$\frac{L}{\lambda_{s2}} = \frac{1}{2\left[\dfrac{C_{s2}}{v_o} - \dfrac{C_{s2}}{v_e}\right]} \tag{17}$$

where $v_e$ and $v_o$ are the phase velocities of the lowest even and odd mode, respectively. From the known values of $v_e/C_{s2}$ and $v_o/C_{s2}$, the normalized coupling length $L/\lambda_{s2}$ may be calculated as a function of $H/\lambda_{s2}$, with the result shown in Fig. 7. The minimum coupling length is seen to be approximately $2\lambda_{s2}$ for a layer thickness of $0.8\lambda_{s2}$ (recall that $H$ is half the layer thickness), $\lambda_{s2}$ being the wavelength of shear waves in the layer.

*4) The Modal Fields:* The transverse equivalent network is useful not only for the derivation of dispersion relations (by means of the transverse resonance condition) but also for the derivation of the modal fields. Equations (3)–(5) furnish the prescription whereby the field components of a particular wave are

related to the voltage and current of its transmission line representation. Since the mode functions $\boldsymbol{g}$ and $\boldsymbol{q}$ are presumed known, the particle velocity $\boldsymbol{v}$ and normal stress $\boldsymbol{z}_0 \cdot \mathfrak{I}$ are fully determined by the voltage and current on the transmission line representation. [Similar remarks pertain to the field components in (5).]

In view of the fact that the modal fields of the Rayleigh type are made up of a combination of the bulk $P$ and $SV$ waves, it follows that

$$\boldsymbol{G} = \boldsymbol{G}_p + \boldsymbol{G}_s = [V_p(z)\boldsymbol{g}_p + V_s(z)\boldsymbol{g}_s]e^{-jk_x x} \quad (18)$$

$$\boldsymbol{Q} = \boldsymbol{Q}_p + \boldsymbol{Q}_s = [I_p(z)\boldsymbol{q}_p + I_s(z)\boldsymbol{q}_s]e^{-jk_x x} \quad (19)$$

where the mode functions $\boldsymbol{g}$ and $\boldsymbol{q}$ for the $P$ and $SV$ waves are given in Table I and the voltages and currents are to be determined from the appropriate equivalent network of Fig. 4, depending on whether the mode in question is even or odd. In either case, the solution for the voltages and currents is a straightforward transmission line problem, the details of which [11] will be omitted. Upon substituting these solutions for the voltages and currents together with the mode functions from Table I into (18) and (19), one obtains the following expressions for the modal fields. For the *even*-mode fields in the *layer* region ($|z| \leq H$), one has

$$v_{x2} = \frac{V_{p2}(0)}{\sqrt{\mu_2\rho_2}}\left[\frac{k_x}{k_{s2}}\cos \kappa_{p2}z - \frac{V_{s2}(0)}{V_{p2}(0)}\cos \kappa_{s2}z\right]e^{-jk_x x} \quad (20)$$

$$v_{y2} = 0 \quad (21)$$

$$v_{z2} = -j\frac{V_{p2}(0)}{\sqrt{\mu_2\rho_2}}\left[\frac{\kappa_{p2}}{k_{s2}}\sin \kappa_{p2}z + \frac{V_{s2}(0)}{V_{p2}(0)}\frac{k_x}{\kappa_{s2}}\sin \kappa_{s2}z\right]e^{-jk_x x} \quad (22)$$

$$T_{zx2} = -jV_{p2}(0)\left[-2\frac{k_x\kappa_{p2}}{{k_{s2}}^2}\sin \kappa_{p2}z + \frac{V_{s2}(0)}{V_{p2}(0)}\frac{{\kappa_{s2}}^2 - {k_x}^2}{k_{s2}\kappa_{s2}}\sin \kappa_{s2}z\right]e^{-jk_x x} \quad (23)$$

$$T_{zy2} = 0 \quad (24)$$

$$T_{zz2} = V_{p2}(0)\left[\frac{{k_x}^2 - {\kappa_{s2}}^2}{{k_{s2}}^2}\cos \kappa_{p2}z - \frac{V_{s2}(0)}{V_{p2}(0)}\,2\,\frac{k_x}{k_{s2}}\cos \kappa_{s2}z\right]e^{-jk_x x}. \quad (25)$$

The voltage $V_{p2}(0)$ is merely the arbitrary constant which occurs in every source-free solution, but the ratio $V_{s2}(0)/V_{p2}(0)$ is determined by the network of Fig. 4(b) (or boundary conditions) and is given by the expression

$$\frac{V_{s2}(0)}{V_{p2}(0)} = -\left[\frac{Z_{p1}Z_{s1} + (a^2Z_{s1} + c^2Z_{p1})(-jZ_{p2}\cot \kappa_{p2}H)}{(abZ_{s1} + cdZ_{p1})(-jZ_{p2}\cot \kappa_{p2}H)}\right] \cdot \frac{\cos \kappa_{p2}H}{\cos \kappa_{s2}H}. \quad (26)$$

For the type of mode being considered, where $\kappa_{s1}$ and $\kappa_{p1}$ are imaginary while $\kappa_{s2}$ and $\kappa_{p2}$ are real, the definition of the characteristic impedances as given in Table I implies that $Z_{s1}$ and $Z_{p1}$ are imaginary while $Z_{s2}$ and $Z_{p2}$ are real. The turns ratios $a$, $b$, $c$, and $d$ are all real and the net result is that the ratio $V_{s2}(0)/V_{p2}(0)$ is real.

In the *substrate* regions ($|z| \geq H$), the fields are exponentially decaying instead of trigonometric, and one has for the *even*-mode fields:

$$v_{x1} = \frac{V_{p1}(-H)}{\sqrt{\mu_1\rho_1}}\left[\frac{k_x}{k_{s1}}e^{-|\kappa_{p1}|(|z|-H)} - \frac{V_{s1}(-H)}{V_{p1}(-H)}e^{-|\kappa_{s1}|(|z|-H)}\right]e^{-jk_x x} \quad (27)$$

$$v_{y1} = 0 \quad (28)$$

$$v_{z1} = \frac{-jV_{p1}(-H)}{\sqrt{\mu_1\rho_1}}\left[\frac{|\kappa_{p1}|}{k_{s1}}e^{-|\kappa_{p1}|(|z|-H)} - \frac{k_x}{|\kappa_{s1}|}\frac{V_{s1}(-H)}{V_{p1}(-H)}e^{-|\kappa_{s1}|(|z|-H)}\right]e^{-jk_x x} \quad (29)$$

$$T_{zx1} = -jV_{p1}(-H)\left[\frac{2k_x|\kappa_{p1}|}{{k_{s1}}^2}e^{-|\kappa_{p1}|(|z|-H)} - \frac{|\kappa_{s1}|^2 + {k_x}^2}{k_{s1}|\kappa_{s1}|}\frac{V_{s1}(-H)}{V_{p1}(-H)}e^{-|\kappa_{s1}|(|z|-H)}\right]e^{-jk_x x} \quad (30)$$

$$T_{zy1} = 0 \quad (31)$$

$$T_{zz1} = V_{p1}(-H)\left[\frac{{k_x}^2 + |\kappa_{s1}|^2}{{k_{s1}}^2}e^{-|\kappa_{p1}|(|z|-H)} - 2\frac{k_x}{k_{s1}}\frac{V_{s1}(-H)}{V_{p1}(-H)}e^{-|\kappa_{s1}|(|z|-H)}\right]e^{-jk_x x}. \quad (32)$$

In this case, the ratio $V_{s1}(-H)/V_{p1}(-H)$ is found from the network of Fig. 4(b) to be

$$\frac{V_{s1}(-H)}{V_{p1}(-H)} = \frac{c(Z_{p2}\cot \kappa_{p2}H) + d(Z_{s2}\cot \kappa_{s2}H)R}{a(Z_{p2}\cot \kappa_{p2}H) + b(Z_{s2}\cot \kappa_{s2}H)R} \quad (33)$$

where

$$R = -\frac{Z_{p1}Z_{s1} + (a^2Z_{s1} + c^2Z_{p1})(-jZ_{p2}\cot \kappa_{p2}H)}{(abZ_{s1} + cdZ_{p1})(-jZ_{s2}\cot \kappa_{s2}H)} \quad (34)$$

and an inspection of (33) and (34) shows that the ratio is real.

The cross-sectional variation of the velocity and stress fields for even modes, as given in (20) through (34), is shown in Figs. 8 and 9 for the case of a gold layer between fused quartz substrates, where $H/\lambda_{s2} = 0.5$ and $\lambda_{s2}$ is the shear-wave wavelength in the gold layer, in which case the $P$ wave constituent in the layer is transversely below cutoff ($\kappa_{p2}$ imaginary).

In a similar fashion, the modal fields of *odd* symmetry are described by the following expressions. In the *layer* region ($|z| \leq H$)

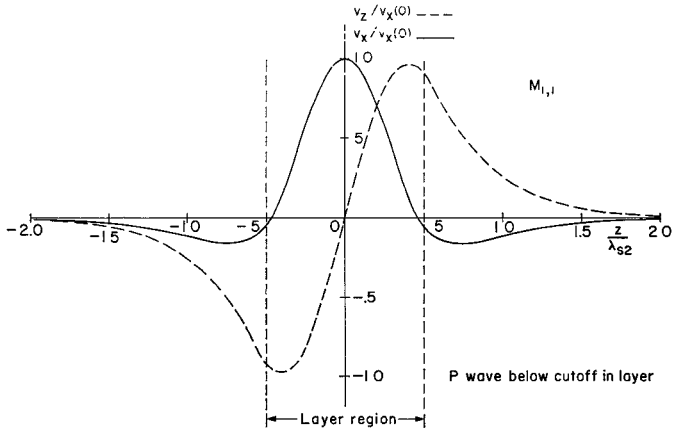


Fig. 8. Particle velocity components for lowest even mode of Rayleigh type.

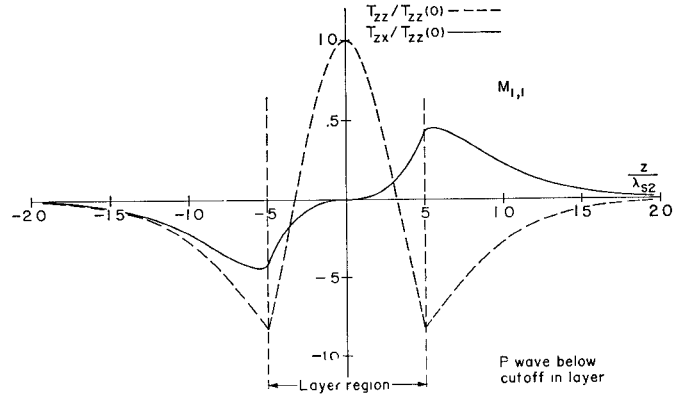


Fig. 9. Stress distribution for lowest even mode of Rayleigh type.

$$v_{x2} = -jI_{p2}(0)\left[\frac{k_x}{\kappa_{p2}}\sin\kappa_{p2}z - \frac{I_{s2}(0)}{I_{p2}(0)}\frac{\kappa_{s2}}{k_{s2}}\sin\kappa_{s2}z\right]e^{-jk_xx} \quad (35)$$

$$v_{y2} = 0 \quad (36)$$

$$v_{z2} = I_{p2}(0)\left[\cos\kappa_{p2}z + \frac{I_{s2}(0)}{I_{p2}(0)}\frac{k_x}{k_{s2}}\cos\kappa_{s2}z\right]e^{-jk_xx} \quad (37)$$

$$T_{zx2} = \sqrt{\mu_2\rho_2}\,I_{p2}(0)\left[-2\frac{k_x}{k_{s2}}\cos\kappa_{p2}z + \frac{I_{s2}(0)}{I_{p2}(0)}\frac{\kappa_{s2}^2 - k_x^2}{k_{s2}^2}\cos\kappa_{s2}z\right]e^{-jk_xx} \quad (38)$$

$$T_{zy2} = 0 \quad (39)$$

$$T_{zz2} = -j\sqrt{\mu_2\rho_2}\,I_{p2}(0)\left[\frac{k_x^2 - \kappa_{s2}^2}{\kappa_{p2}k_{s2}}\sin\kappa_{p2}z - 2\frac{I_{s2}(0)}{I_{p2}(0)}\frac{\kappa_{s2}k_x}{k_{s2}^2}\sin\kappa_{s2}z\right]e^{-jk_xx} \quad (40)$$

where

$$\frac{I_{s2}(0)}{I_{p2}(0)} = -\left[\frac{Z_{p1}Z_{s1} + (a^2Z_{s1} + c^2Z_{p1})(jZ_{p2}\tan\kappa_{p2}H)}{(abZ_{s1} + cdZ_{p1})(jZ_{s2}\tan\kappa_{s2}H)}\right]\cdot\frac{\cos\kappa_{p2}H}{\cos\kappa_{s2}H} \quad (41)$$

is a real quantity.

In the *substrate* region ($|z| \geq H$)

$$v_{x1} = -jI_{p1}(-H)\left[\frac{k_x}{|\kappa_{p1}|}e^{-|\kappa_{p1}|(|z|-H)} + \frac{I_{s1}(-H)}{I_{p1}(-H)}\frac{|\kappa_{s1}|}{k_{s1}}e^{-|\kappa_{s1}|(|z|-H)}\right]e^{-jk_xx} \quad (42)$$

$$v_{y1} = 0 \quad (43)$$

$$v_{z1} = I_{p1}(-H)\left[e^{-|\kappa_{p1}|(|z|-H)} + \frac{I_{s1}(-H)}{I_{p1}(-H)}\frac{k_x}{k_{s1}}e^{-|\kappa_{s1}|(|z|-H)}\right]e^{-jk_xx} \quad (44)$$

$$T_{zx1} = -\sqrt{\mu_1\rho_1}\,I_{p1}(-H)\left[2\frac{k_x}{k_{s1}}e^{-|\kappa_{p1}|(|z|-H)} + \frac{I_{s1}(-H)}{I_{p1}(-H)}\frac{|\kappa_{s1}|^2 + k_x^2}{k_{s1}^2}e^{-|\kappa_{s1}|(|z|-H)}\right]e^{-jk_xx} \quad (45)$$

$$T_{zy1} = 0 \quad (46)$$

$$T_{zz1} = -j\sqrt{\mu_1\rho_1}\,I_{p1}(-H)\left[\frac{|\kappa_{s1}|^2 + k_x^2}{|\kappa_{p1}|k_{s1}}e^{-|\kappa_{p1}|(|z|-H)} + 2\frac{I_{s1}(-H)}{I_{p1}(-H)}\frac{k_x|\kappa_{s1}|}{k_{s1}^2}e^{-|\kappa_{s1}|(|z|-H)}\right]e^{-jk_xx} \quad (47)$$

where

$$\frac{I_{s1}(-H)}{I_{p1}(-H)} = \frac{Z_{p1}[c(Z_{p2}\tan\kappa_{p2}H) + d(Z_{s2}\tan\kappa_{s2}H)R]}{Z_{s1}[a(Z_{p2}\tan\kappa_{p2}H) + b(Z_{s2}\tan\kappa_{s2}H)R]} \quad (48)$$

is real, the quantity $R$ being defined in (34).

The cross-sectional variation of the velocity and stress fields is shown in Figs. 10 and 11 for the lowest odd mode in a gold layer between fused quartz substrates, where $H/\lambda_{s2}=0.8$ and $\lambda_{s2}$ is the shear-wave wavelength in the gold layer. The $P$ wave in the layer is again cut off in this case.

From Figs. 8 to 11 the confinement of the fields to the layer region and the attendant decay into the substrates are clearly seen. It is also noted that the designations of even and odd symmetry are based upon the symmetry of the field components $v_x$ and $T_{zz}$.

### *B. Love-Type Modes*

For the Love or *SH* type of solutions, $v_y$ is the only nonzero component of velocity when $k_y=0$. With respect to the interfaces between the layer and substrate regions, the modal fields may therefore be viewed as being made up of *SH* bulk waves alone.

The transverse equivalent network for the solid–solid interface with *SH* waves incident is also shown in Fig. 3 and this network is combined with the transmission line representation for a bulk *SH* wave to obtain the bisected transverse equivalent networks for Love-type modes of even and odd symmetry, as shown in Fig. 12, where the characteristic impedance $Z_{sh}$ and wavenumber $\kappa_{sh}$ of an *SH* wave are defined in Table I.

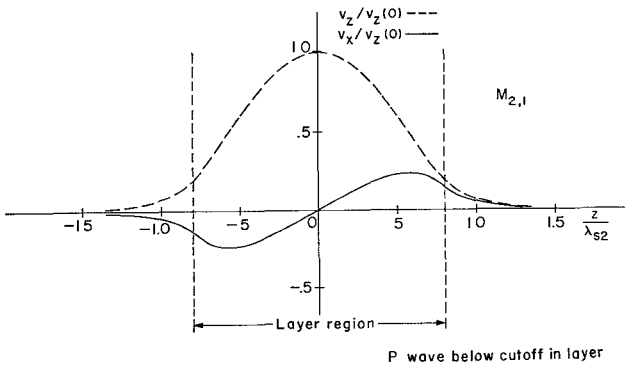


Fig. 10. Particle velocity components for lowest odd mode of Rayleigh type.

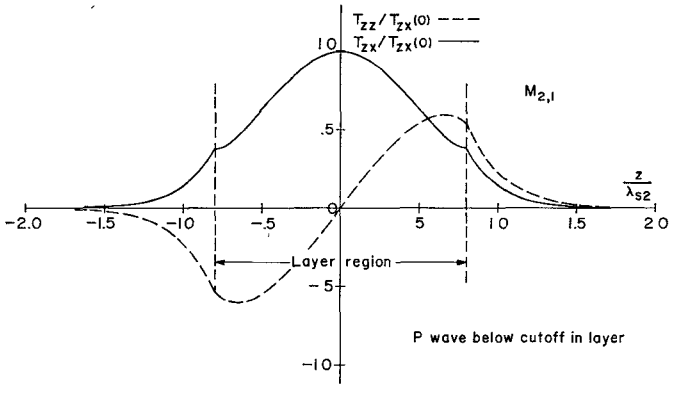


Fig. 11. Stress distribution for lowest odd mode of Rayleigh type.

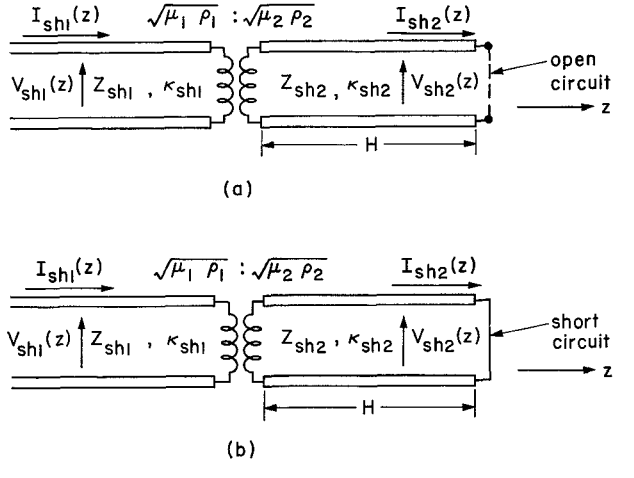


Fig. 12. Bisected transverse equivalent network for Love-type modes of (a) even and (b) odd symmetry in structure of Fig. 2.

*1) Dispersion Relations:* For the equivalent networks of Fig. 12, the transverse resonance condition (6) reduces to the simple expression

$$\overleftarrow{Z} + \overrightarrow{Z} = 0 \tag{49}$$

where $\overleftrightarrow{Z}$ are the input impedances seen looking in opposite directions at any pair of terminals in the network. In the present situation, it is convenient to choose the terminals at the reference plane $z = -H$ in the layer region, such that

$$\overleftarrow{Z}(-H) = \frac{\mu_2\rho_2}{\mu_1\rho_1} Z_{sh1} = \frac{\mu_2\rho_2}{\mu_1\rho_1} \frac{\omega\rho_1}{\kappa_{sh1}} = \frac{\mu_2}{\mu_1} \frac{\omega\rho_2}{\sqrt{k_{s1}^2 - k_x^2}} \tag{50}$$

and

$$\overrightarrow{Z}(-H) = jZ_{sh2} \begin{Bmatrix} \tan \\ -\cot \end{Bmatrix} \kappa_{sh2} H$$

$$= j \frac{\omega\rho_2}{\sqrt{k_{s2}^2 - k_x^2}} \begin{Bmatrix} \tan \\ -\cot \end{Bmatrix} \sqrt{k_{s2}^2 - k_x^2}\, H \begin{matrix} (\text{odd}) \\ (\text{even}) \end{matrix}. \tag{51}$$

Substituting (50) and (51) into (49), one obtains the dispersion relation for Love-type modes:

$$\frac{\mu_2}{\mu_1} \sqrt{k_{s2}^2 - k_x^2}$$

$$= j\sqrt{k_{s1}^2 - k_x^2} \begin{Bmatrix} -\tan \\ \cot \end{Bmatrix} \sqrt{k_{s2}^2 - k_x^2}\, H \begin{matrix} (\text{odd}) \\ (\text{even}) \end{matrix}. \tag{52}$$

Since the solutions sought are those which are transversely propagating in the layer but decaying into the substrate, it is necessary that $k_{s2} \geq k_x \geq k_{s1}$ or, alternatively, $C_{s2} \leq v_p \leq C_{s1}$. In particular, it is necessary that $\sqrt{k_{s1}^2 - k_x^2} = -j\sqrt{k_x^2 - k_{s1}^2}$ in order to represent a decay into the substrates. Consequently, (52) may be rewritten in real form as:

$$\frac{\mu_1}{\mu_2} \sqrt{k_x^2 - k_{s1}^2}$$

$$= \sqrt{k_{s2}^2 - k_x^2} \begin{Bmatrix} -\cot \\ \tan \end{Bmatrix} \sqrt{k_{s2}^2 - k_x^2}\, H \begin{matrix} (\text{odd}) \\ (\text{even}) \end{matrix}. \tag{53}$$

One notes that the dispersion relation for even Love-type modes in the structure with layer thickness $2H$ is identical to that for an actual Love wave on a single substrate covered with a layer of thickness $H$. An inspection of the modal fields to be presented below will also show an identity between these two cases.

Upon identifying the elastic stiffness $\mu$ with the inverse of electromagnetic permeability, a one-to-one correspondence is also found to exist between the Love-type modes of (53) and the electromagnetic $H$-mode surface waves of a dielectric slab of thickness $2H$, where the air region outside the dielectric corresponds to the substrates in the acoustic case. The horizontally polarized electric field $E_y$ in the electromagnetic case corresponds to the particle velocity $v_y$ in the acoustic case. Similarly, $H_x$ corresponds to $T_{yx}$ and $H_z$ to $T_{yx}$.

A numerical solution of (53) for the phase and group velocities is shown in Figs. 13 and 14. The lowest mode is an even mode and propagates down to zero frequency, whereas the lowest odd mode has a finite cutoff frequency.

*2) The Modal Fields:* Since the Love-type modes are made up of bulk $SH$ wave constituents only, the representations (3) and (4) take the form

$$\mathcal{G} = V_{sh}(z)\mathcal{g}_{sh}(x, y) \tag{54}$$

$$\mathcal{Q} = I_{sh}(z)\mathcal{q}_{sh}(x, y) \tag{55}$$

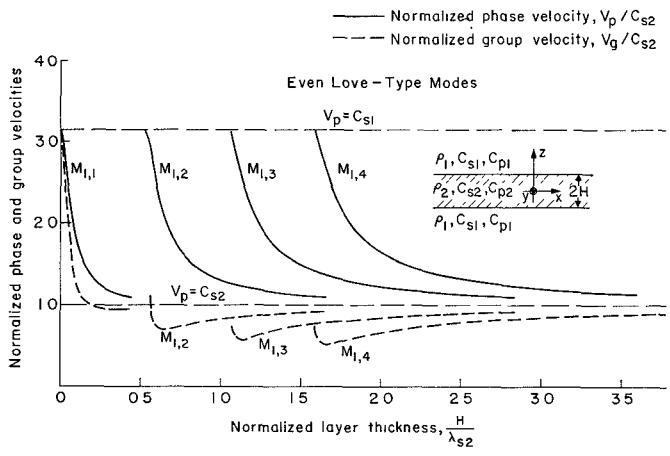


Fig. 13. Dispersion characteristics of even Love-type modes in gold layer between fused quartz substrates.

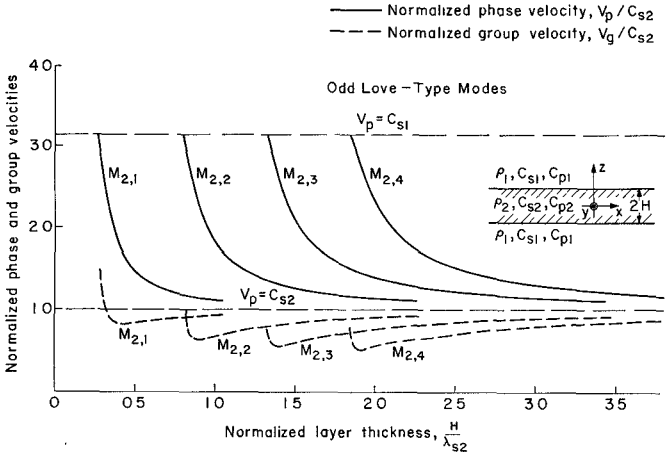


Fig. 14. Dispersion characteristics of odd Love-type modes in gold layer between fused quartz substrates.

where $V_{sh}(z)$ and $I_{sh}(z)$ are the voltage and current on the appropriate transverse equivalent network of Fig. 12, and the bulk wave mode functions $\boldsymbol{g}_{sh}$ and $\boldsymbol{q}_{sh}$ are given in Table I. The solutions for the voltage and current are trivial for the simple networks of Fig. 12 and, combining these with the mode function expressions, one obtains the following modal fields for the Love-type waves. For the fields of the *even* modes, one has:

$$v_{y2} = \frac{V_{sh2}(0)}{\sqrt{\mu_2\rho_2}} \cos \kappa_{sh2} z e^{-jk_x x} \tag{56}$$

$$T_{zy2} = jV_{sh2}(0) \frac{\kappa_{sh2}}{k_{s2}} \sin \kappa_{sh2} z e^{-jk_x x} \tag{57}$$

$$v_{y1} = \frac{V_{sh2}(0)}{\sqrt{\mu_2\rho_2}} \cos \kappa_{sh2} H e^{-|\kappa_{sh1}|(|z|-H)} e^{-jk_x x} \tag{58}$$

$$T_{zy1} = jV_{sh2}(0) \frac{\kappa_{sh2}}{k_{s2}} \sin \kappa_{sh2} H e^{-|\kappa_{sh1}|(|z|-H)} e^{-jk_x x} \tag{59}$$

where the subscripts 1 and 2 distinguish between substrate and layer, respectively.

Similarly, for the *odd*-mode fields, one has:

$$v_{y2} = -jI_{sh2}(0) \frac{k_{s2}}{\kappa_{sh2}} \sin \kappa_{sh2} z e^{-jk_x x} \tag{60}$$

$$T_{zy2} = -I_{sh2}(0)\sqrt{\mu_2\rho_2} \cos \kappa_{sh2} z e^{-jk_x x} \tag{61}$$

$$v_{y1} = -jI_{sh2}(0) \frac{k_{s2}}{\kappa_{sh2}} \sin \kappa_{sh2} H e^{-|\kappa_{sh1}|(|z|-H)} e^{-jk_x x} \tag{62}$$

$$T_{zy1} = -I_{sh2}(0)\sqrt{\mu_2\rho_2} \cos \kappa_{sh2} H e^{-|\kappa_{sh1}|(|z|-H)} e^{-jk_x x}. \tag{63}$$

In view of the simplicity of these Love-type solutions, figures for their transverse dependence [11] are omitted.

## III. Conclusion

The use of a solid layer between two substrates is proposed as a means of coupling Rayleigh wave energy from one substrate to the other, especially when piezoelectricity is absent from one or both of the substrates, in which case air-gap coupling cannot be used. To aid in the understanding and design of such a solid-layer coupler, the characteristic modes of the layered region have been investigated in detail for the case of two identical substrates, and a coupling length which yields optimum transfer of energy from one substrate to the other is computed for a layer of typical thickness.

## Appendix

### Condition for Optimum Power Transfer Between Two Identical Solids

Let a Rayleigh wave of unit amplitude, propagating on the lower substrate, be incident on the layered region, as shown in Fig. 1(b). Such a Rayleigh wave on the lower substrate may be regarded as a superposition of two separate pairs of Rayleigh waves. In the first pair, identical Rayleigh waves are incident on the upper and lower substrates, while in the second pair, the Rayleigh wave on the upper substrate is phase-reversed with respect to that on the lower substrate. Mathematically, this superposition may be represented by the following equation:

$$\begin{pmatrix}0\\1\end{pmatrix} = \frac{1}{2}\begin{pmatrix}1\\1\end{pmatrix} + \frac{1}{2}\begin{pmatrix}-1\\1\end{pmatrix} \tag{A.1}$$

where the upper and lower elements in the column vectors represent the amplitudes of the Rayleigh waves on the upper and lower substrates, respectively. The (1, 1) excitation is of even symmetry with respect to the midplane of the structure while the (−1, 1) excitation is odd. These excitations therefore excite the even and odd modes of the layered region, respectively. Let the amplitude of the lowest of each such mode, due to the excitation given in (A.1), be $S_e$ and $S_o$, where the subscripts $e$ and $o$ denote even and odd. Assuming the design to be such that all higher modes are evanescent, only the above two modes propagate to the "output" end of the layer, where their amplitudes become

$S_e e^{-jk_{xe}L}$ and $S_o e^{-jk_{xo}L}$, $L$ being the length of the layer. If $S_e$ and $S_o$ are the elements of an appropriately normalized scattering matrix, then the reciprocity of the structure implies that the scattering matrix is symmetrical, so that $S_e$ is also the appropriate scattering coefficient from the even mode of the layer to the even distribution of Rayleigh waves on the substrates beyond the layer, and similarly for $S_o$. As a result, the Rayleigh wave fields beyond the "output" of the layer are represented by the vector

$$\frac{1}{2}S_e^2 e^{-jk_{xe}L}\begin{pmatrix}1\\1\end{pmatrix}+\frac{1}{2}S_o^2 e^{-jk_{xo}L}\begin{pmatrix}-1\\1\end{pmatrix}$$
$$=\frac{1}{2}S_e^2 e^{-jk_{xe}L}\left[\begin{pmatrix}1\\1\end{pmatrix}+\frac{S_o^2}{S_e^2}e^{-j(k_{xo}-k_{xe})L}\begin{pmatrix}-1\\1\end{pmatrix}\right]. \quad \text{(A.2)}$$

If the "aperture" field at the cross section containing the beginning of the layer is approximated by the field of the incident Rayleigh wave, the scattering coefficients $S_e$ and $S_o$ must then be real quantities because these coefficients are essentially the projection of the real aperture (Rayleigh wave) field on the modes of the layer, which are likewise real in their transverse field distribution. In practice, bulk waves are generated at the input and output junctions and these will contribute to the aperture field, but their effect is probably small.

Within the above approximation, therefore, the optimum transfer of energy from the lower to upper substrates is seen from (A.2) to occur when

$$(k_{xo} - k_{xe})L = \pi.$$

The ratio of energy on the upper and lower substrates is then given by:

$$\frac{P_u}{P_l}=\frac{|1+S_o^2/S_e^2|^2}{|1-S_o^2/S_e^2|^2}.$$

Complete transfer of energy can occur only if $S_o = S_e$, but this will not in general be the case. Nevertheless, the asymmetry of a single Rayleigh wave propagating on one substrate is such that neither of the layer modes is preferentially excited to any significant degree, so that one would expect $S_o$ and $S_e$ to be of comparable magnitude.

## References


[1] W. L. Bond *et al.*, "Acoustic surface wave coupling across an air gap," *Appl. Phys. Lett.*, vol. 14, Feb. 15, 1969.
[2] A. P. Van Den Heuvel, D. B. Owen, and S. G. Joshi, "Hybrid transducer: A new technique for generating surface waves on non-piezoelectric substrates," presented at the IEEE G-SU Ultrasonics Symp., St. Louis, Mo., Paper C-8, Sept. 1969.
[3] W. C. Wang, P. Staecker, and R. C. M. Li, "Elastic waves bound to a fluid layer between two adjacent solids," *Appl. Phys. Lett.*, vol. 16, no. 8, Apr. 15, 1970.
[4] A. A. Oliner, "Microwave network methods for guided elastic waves," *IEEE Trans. Microwave Theory Tech. (Special Issue on Microwave Acoustics)*, vol. MTT-17, pp. 812–826, Nov. 1969.
[5] A. A. Oliner, H. L. Bertoni, and R. C. M. Li, "A microwave network formalism for acoustic waves in isotropic media," to be published.
[6] A. A. Oliner, R. C. M. Li, and H. L. Bertoni, "A catalog of acoustic equivalent networks for planar interfaces," to be published.
[7] A. A. Oliner, R. C. M. Li, and H. L. Bertoni, "Microwave network approach to guided acoustic surface wave structures," Final Rep. ECOM-0418-F, Polytechnic Inst. Brooklyn, Farmingdale, N. Y., Rep. PIBEP-71-092, Aug. 1971.
[8] G. K. Sezawa and K. Kanai, "Rayleigh waves in an internal stratum," *Bull. Earthquake Res. Inst.*, vol. 10, 1928.
[9] H. I. Tolstoy and E. Usdin, "Dispersive properties of stratified elastic and liquid media: A ray theory," *Geophysics*, vol. 18, 1953.
[10] L. B. Felsen, "Rays, modes, and equivalent networks," *IEEE Trans. Microwave Theory Tech.* (Corresp.), vol. MTT-19, pp. 107–109, Jan. 1971.
[11] A. A. Oliner, R. C. M. Li, and H. L. Bertoni, "Microwave network approach to guided acoustic surface wave structures," 2nd Int. Rep. ECOM-0418-2, Polytechnic Inst. Brooklyn, Farmingdale, N. Y., Rep. PIBEP-70-067, Sept. 1970.


# Short Papers

## Stripline Triplexer for Use in Narrow-Bandwidth Multichannel Filters

RALPH KIHLÉN

*Abstract*—**Design techniques and equivalent circuits are presented for constructing a printed-circuit narrow-bandwidth complementary triplexer filter. The techniques and circuits described allow the construction of contiguous-band multichannel filters using printed circuits with no shorted stubs.**

**A unit was designed and constructed to give a three-percent relative bandwidth for each separate channel. The agreement between theory and experiment was in the range of measurement accuracy.**

Manuscript received September 20, 1971; revised November 11, 1971.
The author is with the Division of Network Theory, Chalmers University of Technology, Gothenburg 5, Sweden.

### Introduction

The design of a multichannel filter requires a network that will separate a given frequency band into $N$ channels with minimum insertion loss and low VSWR at the input port. One way of solving this problem is to use cascaded-channel-separating units [1]–[3], i.e., diplexers, with constant input-port impedances. The advantage of this design is discussed by Matthaei and Cristal [1]. For each channel to be separated, one diplexer is needed. In order to reduce the number of separating units, the author has constructed a triplexer: a unit that separates out two contiguous channels. The total number of elements in a triplexer is the same as in two corresponding diplexers. However, the required space for a triplexer is less than that of two diplexers. The triplexer is a complementary or pseudo-complementary filter unit with constant input-port impedance and it can therefore be cascaded, as the diplexer, to obtain a multichannel filter system of various sizes without any interaction between the filter channels.